A density functional theory study on the rearrangements of the 6-tricyclo[3.2.1.0^{2,4}]octyl cation and its isomers: a walk on the $C_8H_{11}^+$ potential energy surface and a peek at molecular structures with AIM

Nick Henry Werstiuk* and Yi-Gui Wang

Department of Chemistry, McMaster University, Hamilton, Ontario, L8S 4M1, Canada
E-mail: werstiuk@mcmaster.ca

Dedicated to Oswald S. Tee on the occasion of his 60th birthday, and for his contributions to chemistry in Canada

(received 20 Jul 01; accepted 07 Feb 02; published on the web 15 Feb 02)

Abstract

To fully rationalize the solvolytic results of five brosylates (exo,exo-, exo,endo-, and endo,exo-6-tricyclo[3.2.1.0^{2,4}]octyl brosylates **1**-OBs, **2**-OBs, and **3**-OBs, nortricyclyl-3-carbinyl brosylate (**4**-OBs), and 4-tricyclo[3.2.1.0^{2,7}]octyl brosylate (**5**-OBs)) we carried out a DFT (Becke3PW91/6-311G(d,p)) computational study on the C8 H11$^+$ potential energy surface. Four key intermediate cations **9**, **11**, and **13** and their rearrangements are sufficient to account for the experimental results. It is not necessary to envoke so-called memory effects. A peek at the molecular structures of the cations with AIM (Atoms in Molecules) indicates that none of the intermediate cations have penta-coordinate carbons, so they are classical species.

Keywords: Density functional theory, brosylates, Atoms in Molecules (AIM)

Introduction

Isomeric brosylates **1**-OBs**,** **2**-OBs and **3**-OBs have been shown to yield virtually identical mixtures of the four acetates **1**-OAc, **4**-OAc, **5**-OAc and **6**-OAc upon solvolysis.[1,2] The closely related nortricyclyl-3-carbinyl brosylate (**4**-OBs) also gave the same products.[3] On the other hand, tricyclo[3.2.1.0^{2,7}]octan-4-yl brosylate (**5**-OBs) gave only **5**-OAc, **6**-OAc, and a trace of **7**-OAc.[3] Under relatively mild conditions (HOAc, NaOAc, 50^o), **5**-OBs yielded **5**-OAc, **6**-OAc, a trace of **7**-OAc, and **8**-OAc.[4] When the reaction was carried out at 100^o -the temperature used in the solvolysis of **1**-OBs, **2**-OBs, **3**-OBs, and **4**-OBs -**8**-OAc rearranged to **6**-OAc that is the thermodynamic product. Optically active **1**-OBs and **4**-OBs yielded **1**-OAc and **4**-OAc with almost complete retention of optical purity, **5**-OAc with about 30% retention, and **6**-OAc with complete racemization. In contrast, solvolysis of optically active **5**-OBs was accompanied by

internal return and gave acetates **5**-OAc and **6**-OAc as racemates. In order to explain the results, Berson and co-workers proposed a rather complex reaction scheme that included a large number of intermediates and accounted for he retention of configuration in the products on the basis of memory effects.[3] The so-called nonclassical 6-tricyclo[3.2.1.$0^{2,4}$]octyl cation (**9**) derived directly from **1**-OBs was considered a key intermediate in the solvolysis of **1**-OBs, **2**-OBs, **3**-OBs, and **4**-OBs. To (a) extend our computational studies on the molecular structure of carbocations, (b) gain a quantitative understanding of the $C_8H_{11}^+$ potential energy (PE) surface, and (c) obtain an unified mechanistic picture of these solvolyses, we have carried out a computational study at Becke3PW91/6-311G(d,p) level of theory. The results are reported and discussed in this paper.

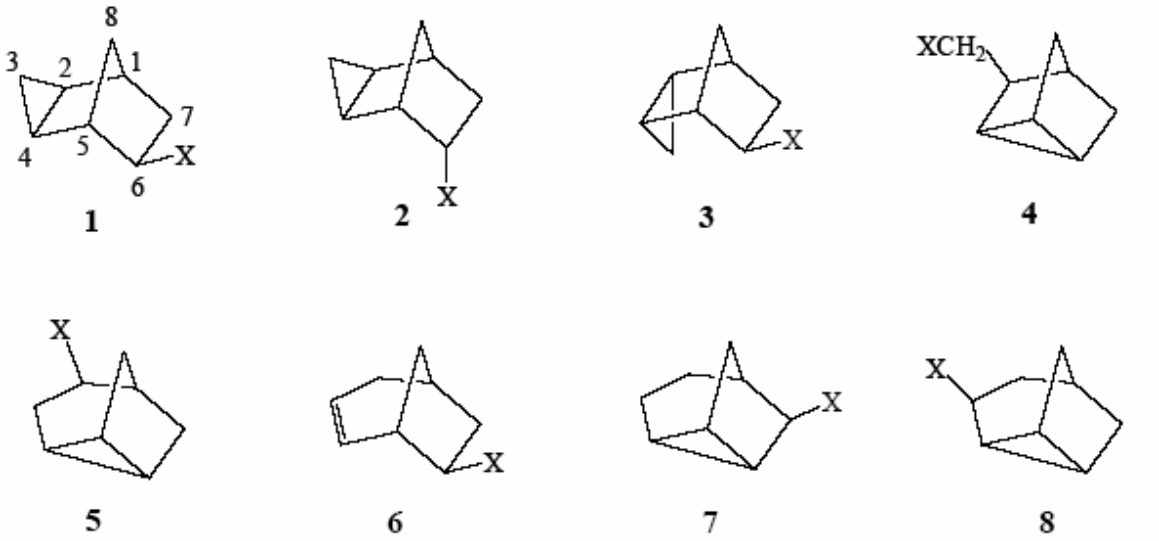

Computational Details

Calculations were carried out with Gaussian94[5] on SGI Octane and SGI 2001 computers and with Gaussian98[6] on a Cray T90. All the geometries and transition states (with OPT=TS) were optimized at the Becke3PW91/6-311G(d,p) level of theory (Table 1 and Table 2). This DFT level was chosen because we established earlier that it yielded results that mirrored those obtained with MP2(full) with the same basis set, but at a much lower computational cost.[7,8] The intrinsic coordinate (IRC) for the rearrangement of **9** to **11** was mapped with sixty points on each side of **TS(9-11)** to ensure it led to **9** and **11**. Zero point energies (ZPVE) were also evaluated at the same level but not scaled. Since Becke3PW91/6-31G(d) has a scaling factor of 0.9774[9], we assumed that the frequencies calculated with a larger basis set have a factor close to 1.0, and consequently did not apply a correction. Solvent field calculations were carried out with Gaussian94 using the SCI-PCM method with a dielectric constant of 6.62 being used for acetic acid (Table 3). ZPVE corrections were not applied in this case. Studies of the topology of the

electron charge density ρ(**r**), integrations over atomic basins, and contour plots were carried out with the AIMPAC suite of programs.[10]

Results and Discussion

Intermediates and reaction mechanisms. Geometry optimizations of the putative cations derived from **1**-OBs and **3**-OBs lead to the same cation **9**. That the cation with the endo cyclopropyl group could not be located as a stationary point strongly indicates that it is not formed as discrete intermediate in the solvolysis of **3**-OBs. This was also the case for the primary cation derived from **4**-OBs. Its fate was determined by the conformation of the $-CH_2^+$ group; when the optimization was initiated from $\mathbf{4}^+\mathbf{a}$, cyclopropyl group participation yielded **9**. When $\mathbf{4}^+\mathbf{b}$ was used as the starting point, the tertiary cyclopropylcarbinyl cation was formed via a 1,2-hydride shift. That the corresponding tertiary acetate is not found as a product indicates that the solvolysis of **4**OBs proceeds preferentially via a conformation that facilitates cyclopropyl participation to yield **9**. By fixing the geometries we estimated the energies of the un-rearranged cations derived from **3**-OBs and **4**-OBs to be at least 11.3 and 18.4 kcal mol^{-1} higher in energy than **9**, respectively. In going from tricyclo[3.2.1.$0^{2,4}$]octane – the parent hydrocarbon – to **9**, the C4-C6 inter-nuclear distance decreased from 2.446 to 1.697 Å. There are other major changes. The C2-C4 and C3-C4 distances are significantly lengthened (1.618 and 1.634 Å, respectively) relative to the hydrocarbon (1.519 and 1.504 Å, respectively).

Table 1. Selected inter-atomic distances (Å) of cations and transition states

	9	**10**	**11**	**12**	**13**	**14**	**TS(9-11)**	**TS(11-13)**	**TS(11-14)**
C1-C2	1.531	1.513	1.394	1.428	1.524	1.563	1.469	1.467	1.496
C1-C7	1.534	1.557	1.843	1.589	1.545	1.485	1.572	1.558	1.520
C2-C7	2.338	2.470	1.843	2.413	2.483	2.399	2.294	2.479	1.807
C2-C3	1.423	1.502	1.497	1.443	1.468	1.539	1.412	1.409	1.504
C2-C4	1.618	1.510	2.428	2.466	2.469	2.545	2.133	2.449	2.429
C3-C4	1.634	1.504	1.515	1.495	1.367	1.504	1.631	1.470	1.519
C4-C5	1.559	1.495	1.505	1.520	1.642	1.432	1.500	1.543	1.493
C4-C6	1.697	2.503	1.506	1.520	1.642	1.682	1.532	1.529	1.529

Table 1. Continued

C5-C8	1.524	1.793	1.515	1.502	1.507	1.518	1.527	1.505	1.514
C6-C8	2.356	1.840	2.495	2.430	2.392	2.480	2.427	2.426	2.470
C5-C6	1.451	1.401	1.506	1.497	1.433	1.615	1.499	1.488	1.524
H12-C2	2.166	2.202	2.140	2.061	1.102	2.190	2.127	1.521	2.159
H12-C3	1.085	1.083	1.092	1.109	2.091	1.091	1.086	1.212	1.092
H16-C2	2.594	2.619	2.117	2.642	2.681	1.094	2.505	2.722	1.345
H16-C7	1.092	1.092	1.095	1.093	1.092	2.639	1.092	1.095	1.271

Table 2 Total energies (E_T, a.u.), zero point vibration energies (ZPVE, kcal/mol^{-1}), number of imaginary frequencies (NIMAG), and relative energies (ΔE, kcal/mol^{-1}) at the B3PW91/6-311G(d,p) level

Cation /TS	ET	ZPVE	NIMAG	ΔE
9	-311.102561	106.7	0	0.0
10	-311.077175	106.1	0	15.3
11	-311.115114	106.3	0	-8.3
12	-311.110979	105.2	1	-6.8
13	-311.141800	106.3	0	-25.0
14	-311.129449	106.6	0	-16.9
TS(9-10)	-311.074708	105.4	1	16.2
TS(9-11)	-311.091486	106.1	1	6.4
TS(11-13)	-311.106518	104.9	1	-4.3
TS(11-14)	-311.103451	105.5	1	-1.8

Table 3. Total energies (E_T,a.u.) and relative energies (ΔE, kcal/mol^{-1}) of **11** and **12** in the acetic acid solvent field without ZPVE corrections

calculation level	ET **11**	ET **12**	ΔE **12-11**
gas phase[a]	-311.115114	-311.110979	2.6
SCI-PCM[b]	-311.187925	-311.183708	2.6
SCI-PCM[c]	-311.135609	-311.131397	2.6

[a] From Table 2. [b]Single point calculations at the Becke3PW91/6-311G(d,p) level on the gas phase geometries. [c]Optimized in the solvent field at the Becke3PW91/6-31G(d,p) level.

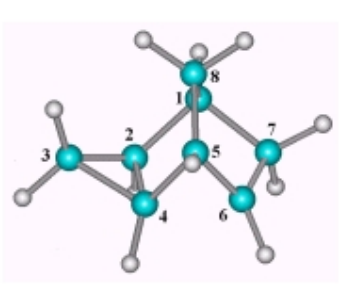

9

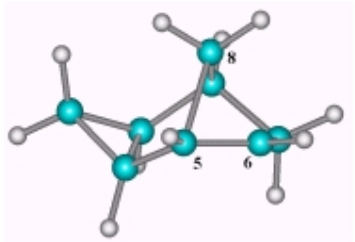

10

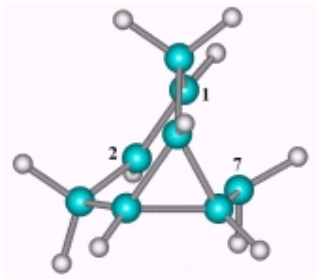

11

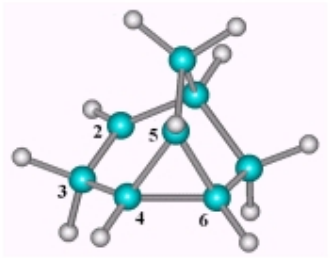

12

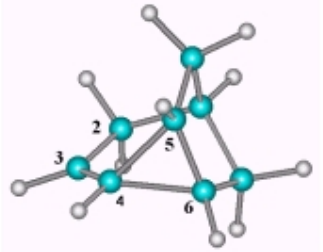

13

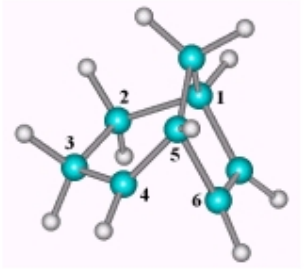

14

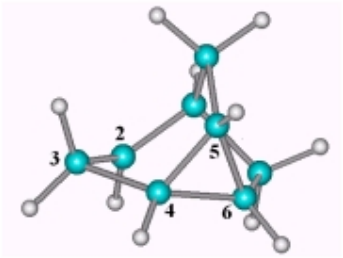

TS(9-11)

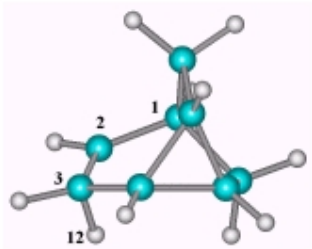

TS(11-13)

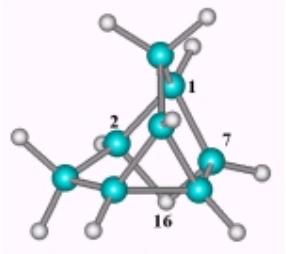

TS(11-14)

These changes are in accord with the fact that a homoconjugative interaction involving the cyclopropyl group is present in **9**.[11] Meanwhile, the C2-C3 and C5-C6 distances decrease, suggesting the development of double-bond character at these centers. In the hydrocarbon, the C-C distances of the cyclopropyl group are all 1.502 Å. We also studied the cation that is the putative intermediate formed by participation of the C5-C8 bond in the solvolysis of the endo brosylate **2**-OBs. This cation (**10**) that is a local minimum on the PE surface is 15.3 kcal mol^{-1} higher in energy than **9** and exhibits a very low barrier for rearrangement to **9** (Scheme 1). Optimization of the cation derived from **5**-OBs yields the Cs cation **11** as the equilibrium geometry with the C1-C7 and C2-C7 distances both being 1.843 Å. This cation that is formed through participation of the C1C7 bond, is 8.3 kcal mol^{-1} lower in energy than **9** after the ZPVE corrections are included. When forced to maintain the appropriate symmetry, cation **12**, the putative secondary "classical" intermediate of Cs symmetry derivable from **5**-OBs is only 1.5 kcal mol^{-1} higher in energy than **11**when ZPVE corrections are applied. Cation **12** possesses an imaginary frequency; the vibrational mode indicates that it is the transition state for the degenerate rearrangement involving **11** and **11**'. Given that **11** and **12** are very close

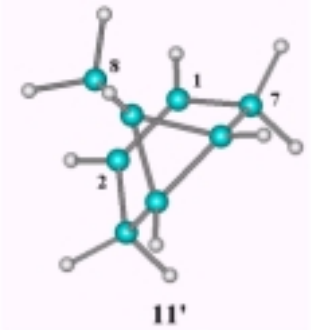

11'

in energy, we carried out calculations in the acetic acid solvent field to establish whether solvation alters ΔET to an extent that the relative energies are reversed. As the data in Table 3 show, solvation does not alter the equilibrium even though the cations are stabilized by >40 kcal mol^{-1} in the acetic acid solvent field. Transition state **TS(9-11)** with ΔET being 6.4 kcal mol^{-1}, was located for the rearrangement of **9** to **11**. That **TS(9-11)** connects **9** and **11** was supported by the nature of vibrational mode corresponding to the imaginary frequency and the IRC calculation. Cation **13** that can be derived directly from **6**-OBs is the most stable species of the C8H**11** $^{+}$ manifold of cations being studied. It has Cs symmetry and is 25.0 kcal mol^{-1} lower in energy than **9**. The C4-C5 and C4-C6 distances are 1.642 Å indicating that **13** is best described as a cyclopropyl carbinyl species. It can also be formed from **11** via a 1,2-hydride shift as shown as **TS(11-13)**. The barrier for this rearrangement is 4.0 kcal mol^{-1}. Cation **11** can also undergo a 1,3-hydride shift to yield cation **14** -see **TS(11-14)** - with a barrier that is 2.5 kcal mol^{-1} higher than the barrier for the 1,2-shift. That acetate 7-OAc is only obtained in trace quantities in the solvolysis of **4**-OBs and **5**-OBs validates the computational results. That the 7-bicyclo[3.2.1]oct-2-enyl cation that is the putative intermediate derivable from **6**-OBs was not located as a

stationary point indicates that it is not an intermediate in the solvolysis of **6**-OBs.

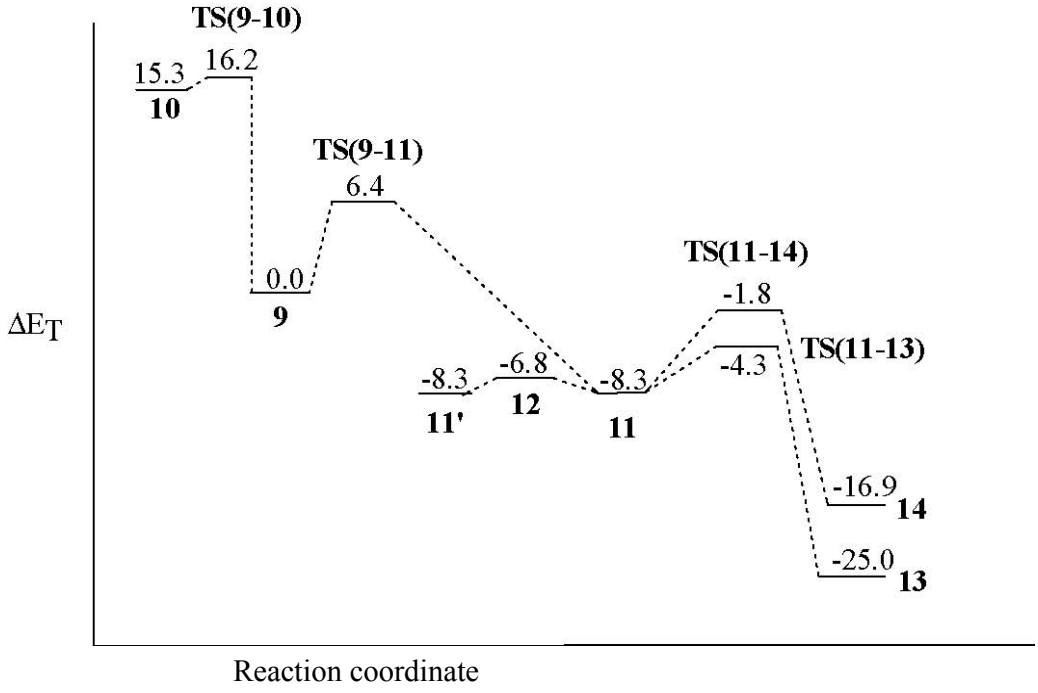

Scheme 1

Of the possible reactive sites in cation **9**, C6 bears the largest positive AIM charge (+0.026) followed by C3 (+0.021). The positive charge on C2 (+0**.**012) is only one-half the charges found on C3 and C6. The C2-C4 and C3-C4 bonds are weak relative to C1-C2 that we take as a normal single bond. These two bonds have relatively small values of the electron density ρ(**r**) (1.250 and 1.196 eÅ^{-3}, respectively) and small values of the Laplacian (-3.452 and –1.859 eÅ^{-5}) at the bond critical points relative to the values (1.635 and -13.060) found for C1-C2; C3-C4 is weaker than C2-C4. Furthermore, both C6 and C3 are less sterically hindered for attack by AcO$^-$than C2. Thus the formation of **1**-OAc – it predominated – and **4**-OAc as the major products with a high degree of retention of configuration from **1**-OBs, **2**-OBs, **3**-OBs, and **4**-OBs is easily rationalized. It is also reasonable to conclude that attack by acetate at C2 of **9** competes with its rearrangement to **11** and this would account for the formation of **5**-OAc (starting from **1**-OBs and and **4**-OBs) with 30% retention of the configuration. Racemic **5**-OAc arises from nucleophilic capture of **11**. Based on our calculations, **5**-OBs will yield cation **11** – not **12** – that rearranges to **13** and **14**. Consequently **5**-OAc and **6**-OAc can only be racemic. Acetate **1**-OAc is not formed from **5**-OBs and **6**-OBs because the barrier for rearrangement of **11** to **9** is 14.7 kcal mol^{-1} (Scheme 1). Acetates **6**-OAc and **8**-OAc can be formed by attack of AcO$^-$at the appropriate methylene and methine carbons of **13**.

In summary, the nature of the products, including stereochemistry, obtained in the solvolysis of **1**-OBs, **2**-OBs, **3**-OBs, **4**-OBs, and **5**-OBs is easily rationalized on the basis of the involvement of only four cations -**9**, **11**, **13**, and **14** -as intermediates. It is not necessary to introduce the concept of a "memory effect".

Molecular structures of cations and transition states. The true connectivity of the atoms – the molecular graphs (structures) - can only be unambiguously determined with AIM by locating bond paths. Cation **9** – a detailed account is documented in a recently accepted publication[11] – does not exhibit a bond path between C4 and C6 as seen in the display of ρ(**r**) and the bond paths at the C4-C5-C6 face (Figure 1). Only one bond was found at C5-C6-C8 face of **10** and it connects C5 to C8. The Cs cation **11**, like the 2norbornyl cation, has a conflict T-structure; that is, a single bond path connects C2 to the (3,-1) bond critical point of the C1-C7 bond. Figure 1 displays ρ(**r**) and bond paths of **11** in the C1-C2-C7 plane. There are two highly curved bond paths between C4 and C5 and C6 of cation **13** in keeping with the fact that it is a cyclopropylcarbinyl species. Figure 1 includes a display of ρ(**r**) and the bond paths of **14** in the C4-C5-C6 plane. It is surprising that in this cation which is also nominally a cyclopropylcarbinyl species, there is no bond path between C4 and C6. This is due to the fact that **14** is an unsymmetrical species in which the C4-C6 inter-nuclear distance (1.682Å) falls near the C4-C6 distance (1.697 Å) of **9**, slightly greater than two of the cyclopropyl C-C distances (1.642Å) of **11**. Figure 1 includes a display of ρ(**r**) and the bond paths in the H-C2-C3 plane of transition state **TS(11-13)**. It is interesting to note that migrating hydrogen H12 is only connected to C3 via a bond path.

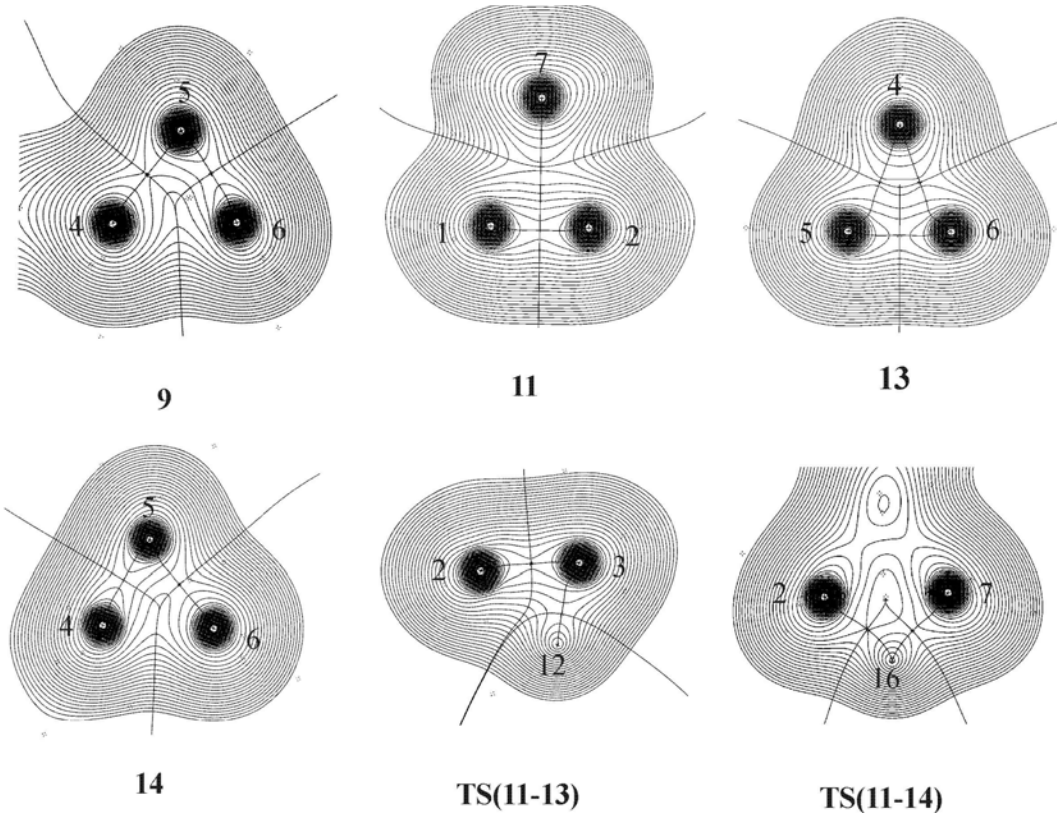

Figure 1. Displays of contours of ρ(**r**) and bond paths at selected faces of intermediates **9, 11, 13, 14** and transition states **TS(11-13) , and TS(11-14).**

As seen in Figure 1, the migrating hydrogen H16 of the 1,3-hydride shift transition state TS(**11-14**) exhibits bond paths to C2 and C7, but there is no bond path between C2 and C7. Thus **TS(11-14)a** and not **TS(11-14)b** is the correct description of the molecular structure of **TS(11-14)** if dashed' lines are used to represent partial bonds. No intermediate included in our study possesses a penta-coordinate carbon. Thus, all the cations are best described as classical species that are stabilized through homoconjugation and delocalization.

TS(11-14)a **TS(11-14)b**

Conclusions

Our computational study at the Becke3PW91/6-311G(d,p) level of theory produced a potential energy surface with four transition states that allowed us to rationalize the experimental results obtained for the solvolysis of five structurally different brosylates on the basis of only four intermediate carbocations. There is no need to envoke a memory effect to account for the results. All the cations of the manifold studied are classical species stabilized by homoconjugation and delocalization.

Acknowledgements

We are indebted to Professor Richard Bader for his stimulating discussions. We acknowledge a grant of CPU time on a CRAY T90 vector computer at the NIC at the Research Center Jülich and the usage of the SGI computing installation in the Geochemistry Labs at McMaster funded by the Natural Sciences and Engineering Research Council of Canada (NSERC). We also thankfully acknowledge a grant of CPU time on a SGI ORIGIN 2000 at the Université de Montréal under the auspices of the Réseau Québécois de Calcul de Haute Performance (RQCHP). We thank NSERC for financial support.

References

1. Wiberg, K. B.; Wenzinger, G. R. *J. Org. Chem.* **1965**, *30*, 2278.
2. Colter, A. K.; Musso, R. C. *J. Org. Chem.* **1965**, *30*, 2462.
3. Berson, J. A.; Bergman, R. G.; Clarke, G. M.; Wege, D. *J. Am. Chem. Soc*. **1969**, *91*, 5601.
4. Berson, J. A.; Wege, D.; Clarke, G.; M. Bergman, R. G. *J. Am. Chem. Soc*. **1969**, *91*, 5594.
5. Frisch, M. J.; Trucks, G. W.; Schlegel, H. B.; Gill, P. M. W.; Johnson, B. G.; Robb, M. A.; Cheeseman, J. R.; Keith, T.; Petersson, G. A.; Montgomery, J. A.; Raghavachari, K.; Al-Laham, M. A.; Zakrzewski, V. G.; Ortiz, J. V.; Foresman, J. B.; Peng, C. Y.; Ayala, P. Y.; Chen, W.; Wong, M. W.; Andres, J. L.; Replogle, E. S.; Gomperts, R.; Martin, R. L.; Fox, D. J.; Binkley, J. S.; Defrees, D. J.; Baker, J.; Stewart, J. P.; Head-Gordon, M.; Gonzalez, C.; Pople, J. A. *Gaussian 94* (Revision B.3), Gaussian, Inc., Pittsburgh PA, 1995.
6. Frisch, M. J.; Trucks, G. W.; Schlegel, H. B.; Scuseria, G. E.; Robb, M. A.; Cheeseman, J. R.; Zakrzewski, V. G.; Montgomery, J. A.; Stratmann, R. E.; Burant, J. C.; Dapprich, S.; Millam, J. M.; Daniels, A. D.; Kudin, K. N.; Strain, M. C.; Farkas, O.; Tomasi, J.; Barone, V.; Cossi, M.; Cammi, R.; Mennucci, B.; Pomelli, C.; Adamo, C.; Clifford, S.; Ochterski, J.; Petersson, G. A.; Ayala, P. Y.; Cui, Q.; Morokuma, K.; Malick, D. K.; Rabuck, A. D.; Raghavachari, K.; Foresman, J. B.; Cioslowski, J.; Ortiz, J. V.; Stefanov, B. B.; Liu, G.; Liashenko, A.; Piskorz, P.; Komaromi, I.; Gomperts, R.; Martin, R. L.; Fox, D. J.; Keith, T.;

Al-Laham, M. A.; Peng, C. Y.; Nanayakkara, A.; Gonzalez, C.; Challacombe, M.; Gill, P. M. W.; Johnson, B. G.; Chen, W.; Wong, M. W.; Andres, J. L.; Head-Gordon, M.; Replogle, E. S. and Pople, J. A. Gaussian 98 (Revision A.1), Gaussian, Inc., Pittsburgh PA, 1998.
7. Werstiuk, N. H.; Muchall, H. M. *J. Mol. Struc. (Theochem)* **1999**, *463*, 225.
8. Werstiuk, N. H.; Muchall, H. M. *J. Phys. Chem. A* **2000**, *104*, 2054.
9. Scott A. P.; Radom L. *J. Phys. Chem.* **1996**, *100*, 16502.
10. Biegler-Konig, F. W.; Bader, R. F. W.; Tang, T.-H. *J. Comput. Chem.* **1982**, *3*, 317.
11. Werstiuk, N. H.; Wang, Y-G. *J. Phys. Chem. A* **2001**, *105*, 11515.

